Title

Critical roles of a small conductance Ca2+-activated K+ channel (SK3) in the repolarization process of atrial myocytes

Journal

Cardiovascular Research, 101(2)

ISSN

1015-5007

Authors

Zhang, Xiao-Dong
Timofeyev, Valeriy
Li, Ning
et al.

Publication Date

2014-02-01

DOI

10.1093/cvr/cvt262

Peer reviewed

Cardiovascular Research (2014) **101**, 317–325
doi:10.1093/cvr/cvt262

Critical roles of a small conductance Ca^{2+}-activated K^+ channel (SK3) in the repolarization process of atrial myocytes

Xiao-Dong Zhang[1†*], Valeriy Timofeyev[1], Ning Li[1], Richard E. Myers[1], Dai-Min Zhang[1,2], Anil Singapuri[1], Victor C. Lau[1], Chris T. Bond[3], John Adelman[3], Deborah K. Lieu[1,4], and Nipavan Chiamvimonvat[1,5*]

[1]Division of Cardiovascular Medicine, University of California, Davis, One Shields Avenue, GBSF 6315, Davis, CA 95616, USA; [2]Department of Cardiology, Nanjing First Hospital, Nanjing Medical University, Nanjing, Jiangsu 21006, P.R. China; [3]Vollum Institute, Portland, OR, USA; [4]Center for Biophotonics, University of California, Davis, Sacramento, CA, USA; and [5]Department of Veterans Affairs, Northern California Health Care System, Mather, CA, USA

Received 19 May 2013; revised 12 November 2013; accepted 17 November 2013; online publish-ahead-of-print 26 November 2013

Time for primary review: 26 days

Aims Small conductance Ca^{2+}-activated K^+ channels ($K_{Ca}2$ or SK channels) have been reported in excitable cells, where they aid in integrating changes in intracellular Ca^{2+} (Ca_i^{2+}) with membrane potentials. We have recently reported the functional expression of SK channels in human and mouse cardiac myocytes. Additionally, we have found that the channel is highly expressed in atria compared with the ventricular myocytes. We demonstrated that human cardiac myocytes expressed all three members of SK channels (SK1, 2, and 3); moreover, the different members are capable of forming heteromultimers. Here, we directly tested the contribution of SK3 to the overall repolarization of atrial action potentials.

Methods and results We took advantage of a mouse model with site-specific insertion of a tetracycline-based genetic switch in the 5′ untranslated region of the *KCNN3* (SK3 channel) gene ($SK3^{T/T}$). The gene-targeted animals overexpress the SK3 channel without interfering with the normal profile of SK3 expression. Whole-cell, patch-clamp techniques show a significant shortening of the action potential duration mainly at 90% repolarization (APD_{90}) in atrial myocytes from the homozygous $SK3^{T/T}$ animals. Conversely, treatment with dietary doxycycline results in a significant prolongation of APD_{90} in atrial myocytes from $SK3^{T/T}$ animals. We further demonstrate that the shortening of APDs in SK3 overexpression mice predisposes the animals to inducible atrial arrhythmias.

Conclusion SK3 channel contributes importantly towards atrial action potential repolarization. Our data suggest the important role of the SK3 isoform in atrial myocytes.

Keywords Small conductance calcium-activated potassium channel • Repolarization • Atrial myocyte • Atrial arrhythmia • Action potential duration

1. Introduction

Small conductance Ca^{2+}-activated K^+ (SK, $K_{Ca}2$) channels were first identified in the central nervous system with sensitivities towards a neurotoxin apamin. The activities of the channels have been shown to affect the intrinsic excitability of neurons, the synaptic transmission, and also synaptic plasticity.[1–4] SK channels are highly unique since the channels are gated solely by submicromolar concentrations of intracellular Ca^{2+}. Hence, the channels function to integrate the intracellular Ca^{2+} concentration into changes in membrane excitability. The SK channel family consists of three members, SK1 ($K_{Ca}2.1$), SK2 ($K_{Ca}2.2$), and SK3 ($K_{Ca}2.3$),[1–3,5,6] encoded by three distinct genes, *KCNN1*, *KCNN2*, and *KCNN3* with different sensitivities towards apamin.[1–3,5–7] SK2 is highly sensitive to apamin, with a half-blocking concentration (IC_{50}) of 60 pmol/L, while the IC_{50} for SK1 channels is ~10 nmol/L.[4,8–10] SK3 channels show intermediate sensitivity.

Our previous studies have demonstrated that SK channels are expressed in human and mouse cardiac myocytes.[11,12] More importantly, we found that SK current contributes significantly to the repolarization process in both mouse and human atria. Further studies in our

† Co-corresponding author.

* Corresponding author. Tel: +1 530 754 7158; fax: +1 530 754 7167. Email: nchiamvimonvat@ucdavis.edu (N.C.) or xdzhang@ucdavis.edu (X.-D.Z.)

laboratory revealed that different members of SK channels exist in human cardiac myocytes, and the channel subunits can heteromultimerize via the coiled-coil domains in the C termini.[13] To probe the mechanism of these channels in the human heart, we have used the yeast two-hybrid screen against the human heart library to identify SK channel interacting partners.[14,15] Our studies have provided unique insights regarding the roles of these newly described channels in the heart.

Our findings have been subsequently supported by several different laboratories.[16–22] Moreover, recent studies using genome-wide association analysis have provided a possible genetic link between *KCNN3* and lone AF in humans.[23,24] Nonetheless, one recent report suggests the lack of contribution of SK channels to cardiac repolarization by demonstrating that SK channels are not active in rat, dog, and human ventricular myocytes and do not contribute to action potential repolarization under normal physiological conditions.[25] Therefore, additional studies are required to further clarify the role of SK channels in cardiac action potential repolarization.

Since the three members of SK channels are expressed in mouse and human cardiomyocytes, we directly tested the contribution of SK3 channels to the overall repolarization of atrial action potentials. We take advantage of a mouse model with site-specific insertion of a tetracycline-based genetic switch in the 5′ untranslated region (UTR) of the gene, so that subunit expression could be decreased by dietary doxycycline (DOX) administration without interfering with the normal profile of SK3 expression. We hypothesize that gain-of-function and loss-of-function of SK3 channels may be sufficient to disrupt the intricate balance of the inward and outward currents during repolarization in atrial myocytes. Here, we demonstrate the important roles of SK3 channels towards the overall repolarization process of atrial myocytes.

2. Methods

2.1 Gene-targeted SK3 mutant mice (*SK3$^{T/T}$*)

All animal care and procedures were approved by the University of California, Davis, Institutional Animal Care and Use Committee. Animal use was in accordance with National Institutes of Health and institutional guidelines. Gene-targeted SK3 mutant mice were previously generated[26] and obtained from Jackson Laboratory (Sacramento, CA, USA; B6.129S4-*Kcnn3^{tm1Jpad}*/J). The *SK3^{T}* mutant allele has a tetracycline-based genetic switch inserted into the 5′ UTR of the *Kcnn3* (SK3) locus, just upstream of the translation initiation site. This genetic switch harbours both the tetracycline-controlled transactivator protein (tTA) and the tetracycline operator [*tetO*; also called tetracycline-responsive element (TRE) or tet-operator]; allowing transcription of the downstream *Kcnn3* locus to be blocked by administration of tetracycline (or its analogue DOX). To suppress SK3 channel expression, DOX was administered to the animals' drinking water (0.5 g/L) for a period of 1 week.[26,27] The mutant mice were maintained as heterozygotes after backcrossing into the C57BL/6J background for more than seven generations. Mutant and wild-type (WT) alleles were confirmed using polymerase chain reaction of tail tissue.[26,27] All chemicals were purchased from Sigma-Aldrich except specifically indicated.

2.2 Analysis of cardiac function by echocardiography

Echocardiograms using M-mode and two-dimensional (2D) measurements to assess systolic function were performed, as described previously, in conscious animals.[28] The measurements represented the average of six selected cardiac cycles from at least two separate scans performed in a random-blind fashion with papillary muscles used as a point of reference for consistency in the level of the scan. End diastole was defined as the maximal left ventricular (LV) diastolic dimension, and end systole was defined as the peak of posterior wall motion. Fractional shortening (FS), a surrogate of systolic function, was calculated from LV dimensions as follows: $FS = [(EDD - ESD)/EDD] \times 100\%$, where EDD and ESD are LV end-diastolic and end-systolic dimensions, respectively.

2.3 RNA extraction and quantitative RT-PCR

Atria and LV free walls were excised from the mouse hearts and homogenized using a Dounce Homogenizer on ice. Since the mouse atrial tissues are very small, we have combined both the left and right atria in the study. Total RNA was isolated using the RNeasy Plus Mini Kit (Qiagen 74134) and cDNA generated using the RT^2 First Strand Kit (Qiagen 330401). cDNA was combined with RT^2 SYBR Green Master Mix (Qiagen 330520) and specific qRT-PCR primers and qRT-PCR analysis run using the Viia^{TM} 7 Real-Time PCR System (ABI). Primer efficiencies were determined by standard dilution curve analysis. A total of three separate samples from three animals for each group were used. The experiments from each sample were performed in triplicate, and average cycle threshold (C_t) values were normalized to GAPDH expression. $\Delta\Delta C_t$ values were determined relative to WT atrial or WT ventricular samples. Fold change was determined as $2^{(-\Delta\Delta C_t)}$. Primers used include *Gapdh* (SA Biosciences PPM02946E), *Kcnn2* (SA Biosciences PPM04196G, Reference sequence: NM_080465), and *Kcnn3* (SA Biosciences PPM04192A, Reference sequence: NM_080466).

2.4 Electrophysiological recordings from WT and SK3$^{T/T}$

Mice were anaesthetized by intraperitoneal injection of pentobarbital (80 mg/kg), and the depth of anaesthesia was assessed by the reaction to toe pinching. Mice were sacrificed by rapid heart excision. Single mouse atrial myocytes were isolated from the right and left atria as previously described[11,28,29] from adult WT and SK3$^{T/T}$ animals from the same littermates at 8–12 weeks of age. Action potentials (APs) were recorded at room temperature using the perforated patch technique at a stimulation frequency of 0.25 Hz.[11,28,29] All other experiments were performed using the conventional whole-cell, patch-clamp technique[30] at room temperature.

For AP recordings, the patch pipettes were backfilled with amphotericin (200 μg/mL). The pipette solution contained (in mM): K-glutamate 120, KCl 25, $MgCl_2$ 1, $CaCl_2$ 1, and *N*-2-hydroxyethylpiperazine-*N*′-2-ethanesulphonic acid (HEPES) 10, pH 7.4 with KOH. The external solution contained NaCl 138, KCl 4, $MgCl_2$ 1, $CaCl_2$ 2, NaH_2PO_4 0.33, glucose 10, and HEPES 10, pH 7.4 with NaOH.

Whole-cell Ca^{2+}-activated K^+ current ($I_{K,Ca}$) was recorded using the conventional voltage-clamp protocol as previously described.[11] The extracellular solution contained (in mM): *N*-methylglucamine (NMG) 140, KCl 4, $MgCl_2$ 1, glucose 5, and HEPES 10, pH 7.4 with HCl. The internal solution consisted of (in mM): potassium gluconate 144, $MgCl_2$ 1.15, EGTA 5, HEPES 10, and $CaCl_2$ yielding a free (unchelated) [Ca^{2+}] of 500 nmol/L using the Calcium Titration Software[31] to calculate free [Ca^{2+}], bound, and dissociated. The pH was adjusted to 7.25 using KOH. All experiments were performed using 3 M KCl–agar bridges. Cell capacitance was also calculated as the ratio of total charge (the integrated area under the current transient) to the magnitude of the pulse (20 mV). Currents were normalized to cell capacity to obtain the current density. The series resistance was compensated electronically. In all experiments, a series resistance compensation of $\geq$90% was obtained. Currents were recorded using an Axopatch 200A amplifier (Axon Instrument, Foster City, CA, USA), filtered at 1 kHz using a four-pole Bessel filter, and digitized at a sampling frequency of 2 kHz. Data analysis was carried out using the Clampfit 10 software and commercially available PC-based spreadsheet and graphics software (MicroCal Origin Pro, version 7.0).

2.5 Electrocardiographic recordings

Electrocardiographic (ECG) recordings were obtained using Bioamplifier (BMA 831, CWE, Inc., Ardmore, PA, USA).[32] The animals were placed on a temperature-controlled warming blanket at 37°C. Four consecutive 2-min epochs of ECG data were obtained from each animal. Signals were low-pass filtered at 0.2 kHz and digitized using Digidata 1200 (Axon Instrument). A total of 100 beats were analysed from each animal in a blinded fashion. The Q−T interval was determined manually by placing cursors on the beginning of the QRS and the end of the T wave. The rate-corrected QT interval (QT_c) was calculated using modified Bazett's formula as reported by Mitchell *et al.*[33] for mouse models, whereby the RR interval was first expressed as a unitless ratio (RR in ms/100 ms). QT_c interval was defined as [QT interval (in ms)/$(RR/100)^{1/2}$].

2.6 *In vivo* electrophysiological studies

In vivo electrophysiological studies were performed as previously described.[34,35] Standard pacing protocols were used to determine the electrophysiological parameters, including sinus node recovery time, atrial, atrioventricular (AV) nodal, and ventricular refractory periods, and also AV nodal conduction properties. Each animal underwent an identical pacing and programmed stimulation protocol.

To induce atrial and ventricular tachycardia and fibrillation, programmed extrastimulation techniques and burst pacing were utilized. Programmed right atrial and right ventricular double and triple extrastimulation techniques were performed at 100-ms drive cycle length, down to a minimum coupling interval of 50 ms. For comparison of the inducibility in each animal, programmed extrastimulation techniques and stimulation duration of atrial and ventricular burst pacing were the same in all mice. Reproducibility was defined as greater than one episode of induced atrial or ventricular tachycardia.

2.7 Statistical analysis

Where appropriate, pooled data are presented as mean ± SEM. Significant differences between groups were tested using analysis of variance with Bonferroni correction using MicroCal Origin, version 7.0. The null hypothesis was rejected when two-tailed *P*-value of <0.05.

3. Results

3.1 Homozygous $SK3^{T/T}$ mice demonstrated overexpression of SK3 transcripts while treatment with DOX resulted in a significant decrease in the SK3 transcripts

Figure 1A shows results of the quantitative reverse transcription polymerase chain reaction (RT-PCR) from the four groups of animals including WT with and without DOX treatment and $SK3^{T/T}$ with and without DOX treatment. Atrial and ventricular tissues were analysed separately. Homozygous $SK3^{T/T}$ mice demonstrate a >50-fold increase in the SK3 mRNA expression in both atrial and ventricular tissues than WT animals ($^*P < 0.05$). In contrast, treatment of the mutant animals with

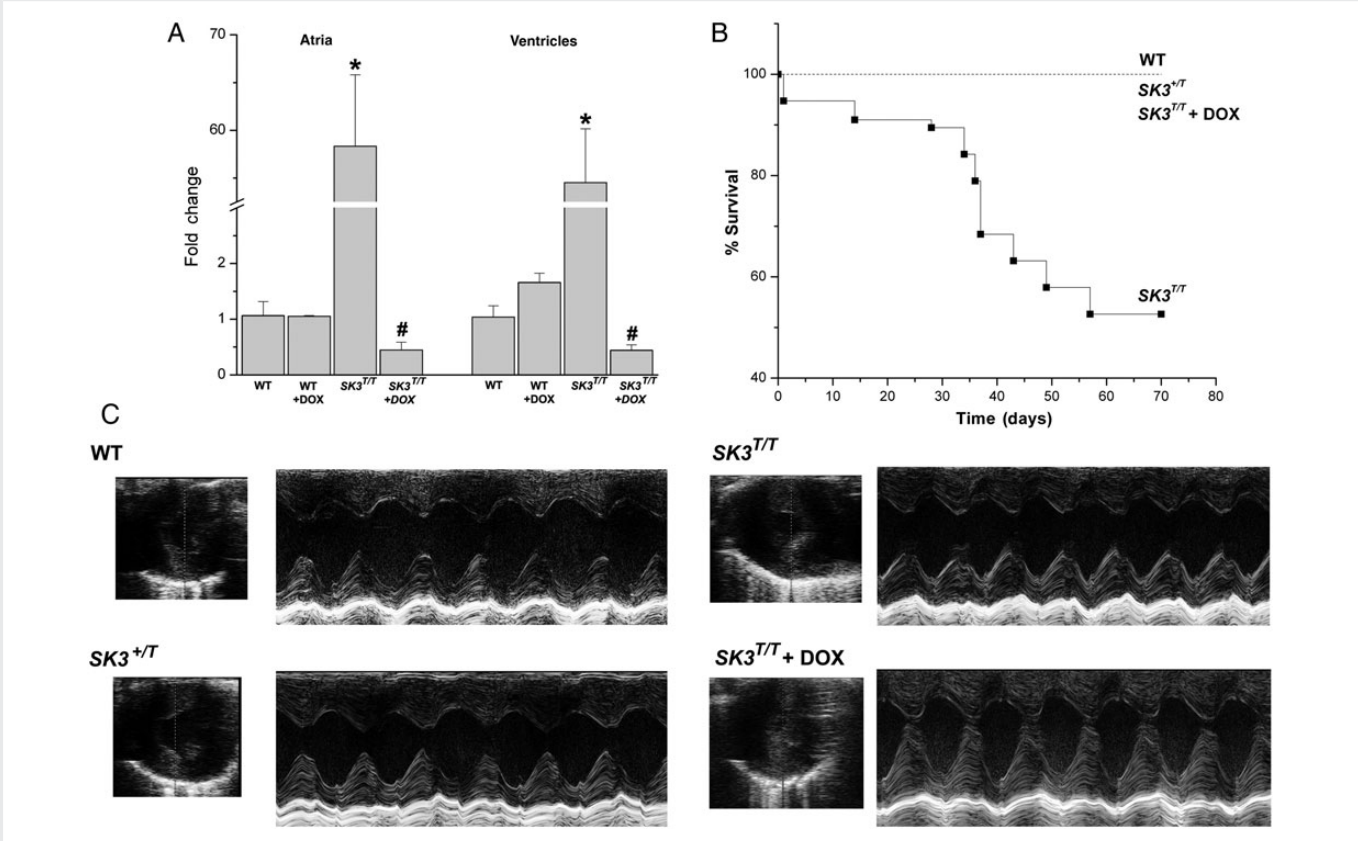

Figure 1 $SK3^{T/T}$ mice showed a significant decrease in survival. (*A*) Quantitative RT-PCR of SK3 channel transcripts from atrial and ventricular tissues from four groups of animals, including $SK3^{T/T}$ with and without DOX treatment compared with WT littermates with and without DOX treatment. (*B*) Survival curves from the four groups of animals. (*C*) Examples of M-mode echocardiography in $SK3^{T/T}$ with and without DOX treatment, $SK3^{+/T}$, and WT littermates. $SK3^{T/T}$ and $SK3^{+/T}$ mice showed no evidence of cardiac abnormalities with normal chamber size and cardiac function.

DOX resulted in a significant decrease in the SK3 channel transcripts to ~0.4-fold of the WT animals ($^{\#}P < 0.05$). The expression of SK2 channel transcripts in both atrial and ventricular tissues are not significantly different among the four groups of animals (see Supplementary material online, *Figure S1*).

3.2 A significant decrease in the survival of homozygous *SK3*$^{T/T}$ mice

SK3$^{T/T}$ mice demonstrated a significant decrease in the survival compared with heterozygous *SK3*$^{+/T}$ or WT littermates (*Figure 1B*). Most of the death occurred suddenly and early after birth within the first 2 months of age.

3.3 Normal cardiac chamber size and function in *SK3*$^{T/T}$ and *SK3*$^{T/T}$ treated with DOX compared with WT animals

Figure 1C shows examples of 2D and M-mode echocardiogram obtained from adult homozygous mutant animals with and without DOX treatment and heterozygous animals compared with WT littermates.

Table 1 Summary of echocardiographic data

Treatment	*N*	EDD (mm)	ESD (mm)	LVPW (D) (mm)	LVPW (S) (mm)	FS (%)
WT	5	2.9 ± 0.1	1.1 ± 0.2	0.9 ± 0.1	1.5 ± 0.1	61.7 ± 4.9
SK3$^{+/T}$	7	3.0 ± 0.1	1.2 ± 0.2	0.8 ± 0.1	1.5 ± 0.1	60.5 ± 4.7
SK3$^{T/T}$	6	3.0 ± 0.2	1.0 ± 0.1	0.8 ± 0.1	1.6 ± 0.1	67.6 ± 4.4
SK3$^{T/T}$ + DOX	3	2.8 ± 0.2	1.0 ± 0.2	1.0 ± 0.04	1.7 ± 0.04	67.7 ± 6.6

Data are mean ± SEM.
EDD, end-diastolic dimension; ESD, end-systolic dimension; LVPW (D), left ventricular posterior wall thickness in diastole; LVPW (S), left ventricular posterior wall thickness in systole.

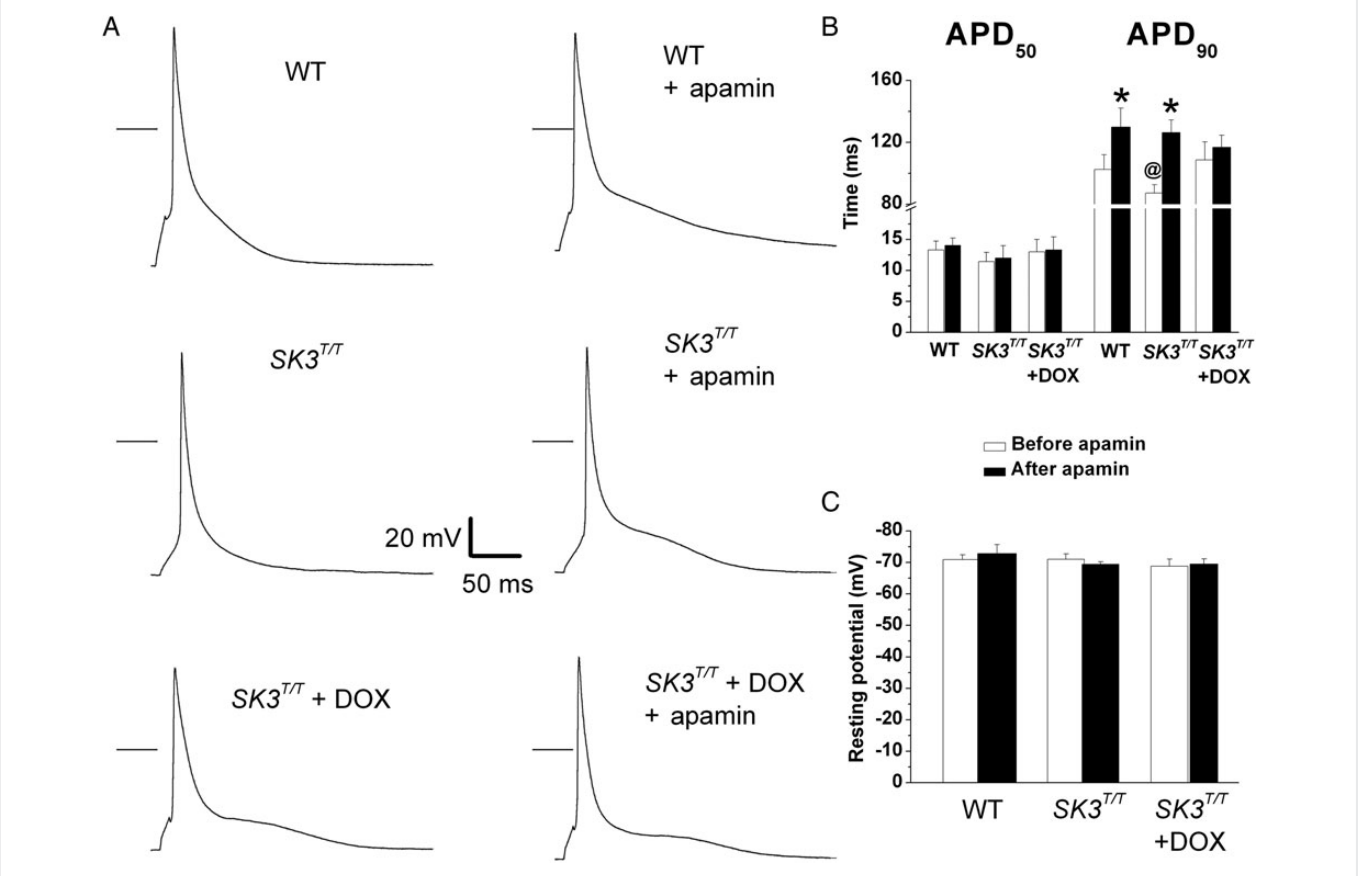

Figure 2 APs recorded from atrial myocytes are shortened in *SK3*$^{T/T}$ and prolonged in *SK3*$^{T/T}$ treated with DOX. (*A*) Examples of APs recorded using the perforated patch-clamp technique from isolated atrial myocytes before and after the application of 10 nmol/L of apamin from three different groups of animals including *SK*$^{T/T}$ with or without DOX and WT littermates. Horizontal bars indicate 0 mV. (*B*) Summary data of APD_{50} and APD_{90} ($^{*}P < 0.05$ comparing before and after apamin, $^{@}P < 0.05$ comparing *SK*$^{T/T}$ with WT littermates and *SK*$^{T/T}$ with DOX treatment, n = a total of 12 cells from five animals for each group). (*C*) Bar graphs show summary data of the resting membrane potentials before and after apamin. Control data are shown as open bars, and data after application of apamin are shown as closed bar.

Overexpression or knockdown of SK3 channels did not significantly alter cardiac chamber size or function. There were no significant differences in the calculated fractional shortening (%FS) from WT, $SK3^{+/T}$, or $SK3^{T/T}$ with or without DOX treatment, respectively. The echocardiographic parameters are summarized in *Table 1*.

3.4 APs recorded from atrial myocytes are shortened in $SK3^{T/T}$ mice

To test the functional roles of SK3 channel in atrial myocytes, we recorded APs from single atrial myocytes isolated from $SK3^{T/T}$ with or without DOX treatment compared with their WT littermate controls using the perforated patch-clamp technique to allow intracellular Ca^{2+} to cycle normally (*Figure 2A*). In addition, APs were recorded using relatively slow pacing frequency at room temperature to accentuate differences between $SK3^{T/T}$ and WT mice. APs were significantly shortened in atrial myocytes isolated from $SK3^{T/T}$ mice compared with their WT littermates. Summary data for action potential duration (APD) at 50 and 90% repolarization (APD_{50} and APD_{90}) at baseline and after apamin from atrial myocytes are shown in *Figure 2B*. Specifically, there was a significant shortening of APD_{90} recorded from atrial myocytes from $SK3^{T/T}$ compared with WT animals (*Figure 2B*, $^{@}P < 0.05$). Treatment of $SK3^{T/T}$ mice with DOX resulted in a significant prolongation of the APD_{90} compared with $SK3^{T/T}$ animals (*Figure 2B*, $^{@}P < 0.05$). Moreover, in contrast to $SK3^{T/T}$ or WT animals, application of apamin resulted in a smaller degree of prolongation of APD_{90} in $SK3^{T/T}$ mice treated with DOX. Overexpression or knockdown of SK3 channel expression did not alter the resting membrane potential of the cardiac myocytes (*Figure 2C*).

3.5 $I_{K,Ca}$ is increased in atrial myocytes isolated from $SK3^{T/T}$ and decreased in $SK3^{T/T}$ treated with DOX compared with WT mice

To further document the basis for the alteration in cardiac AP observed in the mutant animals, we examined whole-cell $I_{K,Ca}$ from single atrial myocytes from $SK3^{T/T}$ mice with and without pre-treatment with DOX and compared with the WT controls. *Figure 3A* shows examples of current traces recorded from atrial myocytes isolated from WT, $SK3^{T/T}$, $SK3^{T/T}$ treated with DOX, respectively. Apamin-sensitive

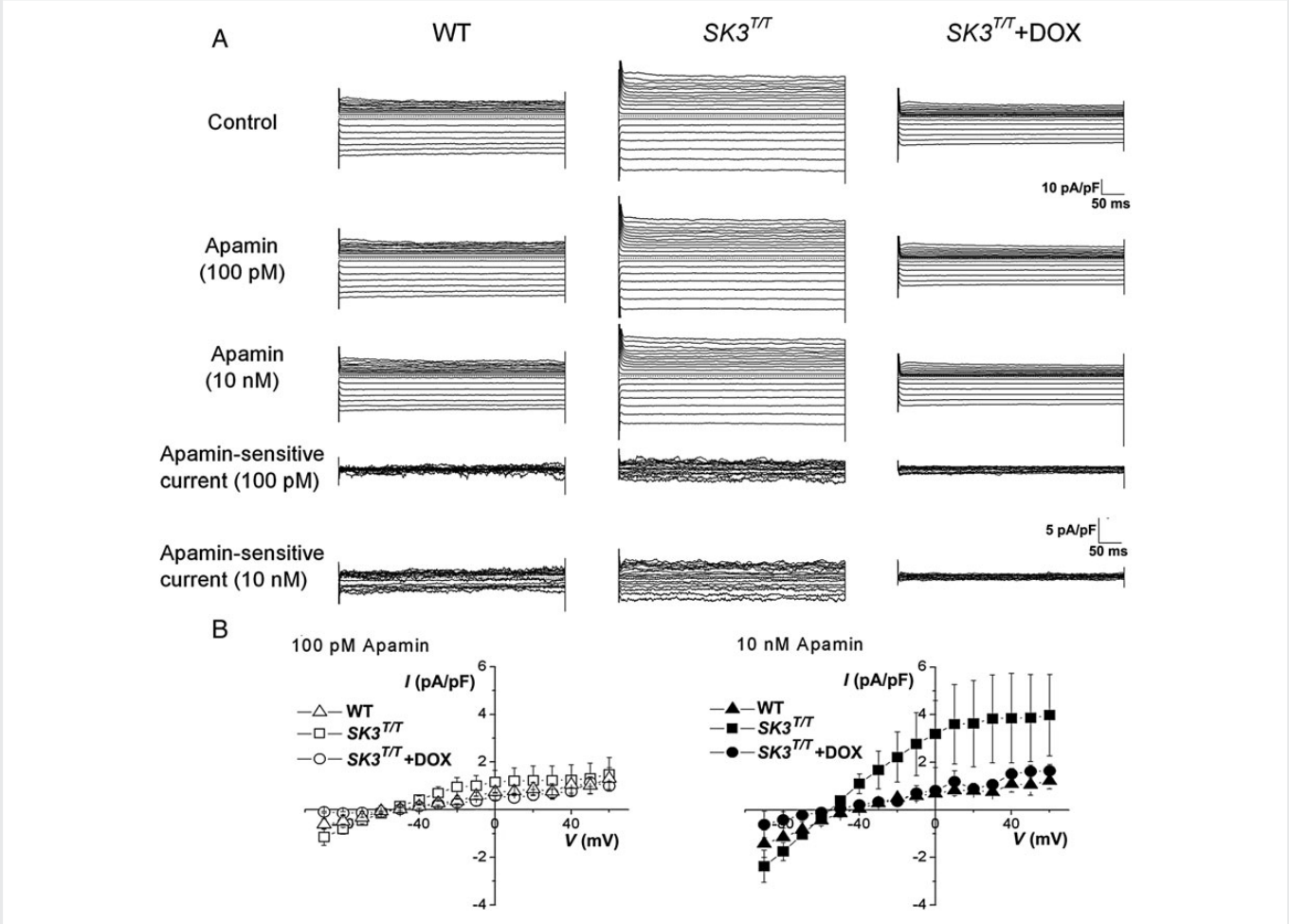

Figure 3 Whole-cell $I_{K,Ca}$ recordings. (*A*) Examples of whole-cell currents recorded from mouse atrial myocytes using voltage steps from a holding potential of −55 mV. The current was recorded in control and after apamin (100 pmol/L and 10 nmol/L), and the free $[Ca^{2+}]_i$ was 500 nmol/L. The apamin-sensitive current traces were obtained using digital subtraction and are shown in the lower panels. (*B*) Current density–voltage relation of the apamin-sensitive current using a concentration of 100 pmol/L and 10 nmol/L, respectively (n = a total of 10–12 cells from 4 to 6 animals for each group).

current ($I_{K,Ca}$) was obtained from subtraction of total current recorded in control and after application of low and high concentrations of apamin (100 pM and 10 nM, respectively). Atrial myocytes isolated from $SK3^{T/T}$ showed a significant increase in the density of $I_{K,Ca}$ compared with the WT littermates (*Figure 3A*). Treatment with DOX in $SK3^{T/T}$ animals resulted in a down-regulation of the $I_{K,Ca}$ density in atrial myocytes compared with the $SK3^{T/T}$. Summary data of the current density–voltage relations from three different groups are shown in *Figure 3B* ($n = 10–12$ cells for each group).

3.6 Functional roles of SK3 channel in intact heart assessed using SK3 overexpression mice

Our previous data have documented the expression of all three members of SK channels in atrial myocytes. However, whether SK3 contributes directly to atrial repolarization in intact animals remains completely unknown. Since $SK3^{T/T}$ mice show an increase in the expression of SK3 channel without alteration in the pattern of expression, we reason that $SK3^{T/T}$ mice will provide an ideal model to study the functional roles of SK3 channel in atria in intact animals. *Figure 4* shows examples of ECG obtained from adult $SK3^{T/T}$ with and without DOX compared with WT littermates. Summary data for the RR, PR, and QT_c intervals are shown in *Figure 4D*. There were no significant differences detected in these three groups of animals. Similarly, the ECG from 4-week-old mice also did not show significant differences among the three groups of animals (see Supplementary material online, *Figure S2*).

The data in *Figure 2* show that overexpression of SK3 channels results in the shortening of atrial APs. We directly test whether abbreviation of the atrial APs may predispose the mutant animals to atrial arrhythmias. *In vivo* electrophysiological studies were performed in *SK3* mutant mice compared with WT animals at 8–12 weeks of age. Consistent with the patch-clamp recordings from atrial myocytes, the atrial effective refractory periods (AERPs) in $SK3^{+/T}$ and $SK3^{T/T}$ are significantly

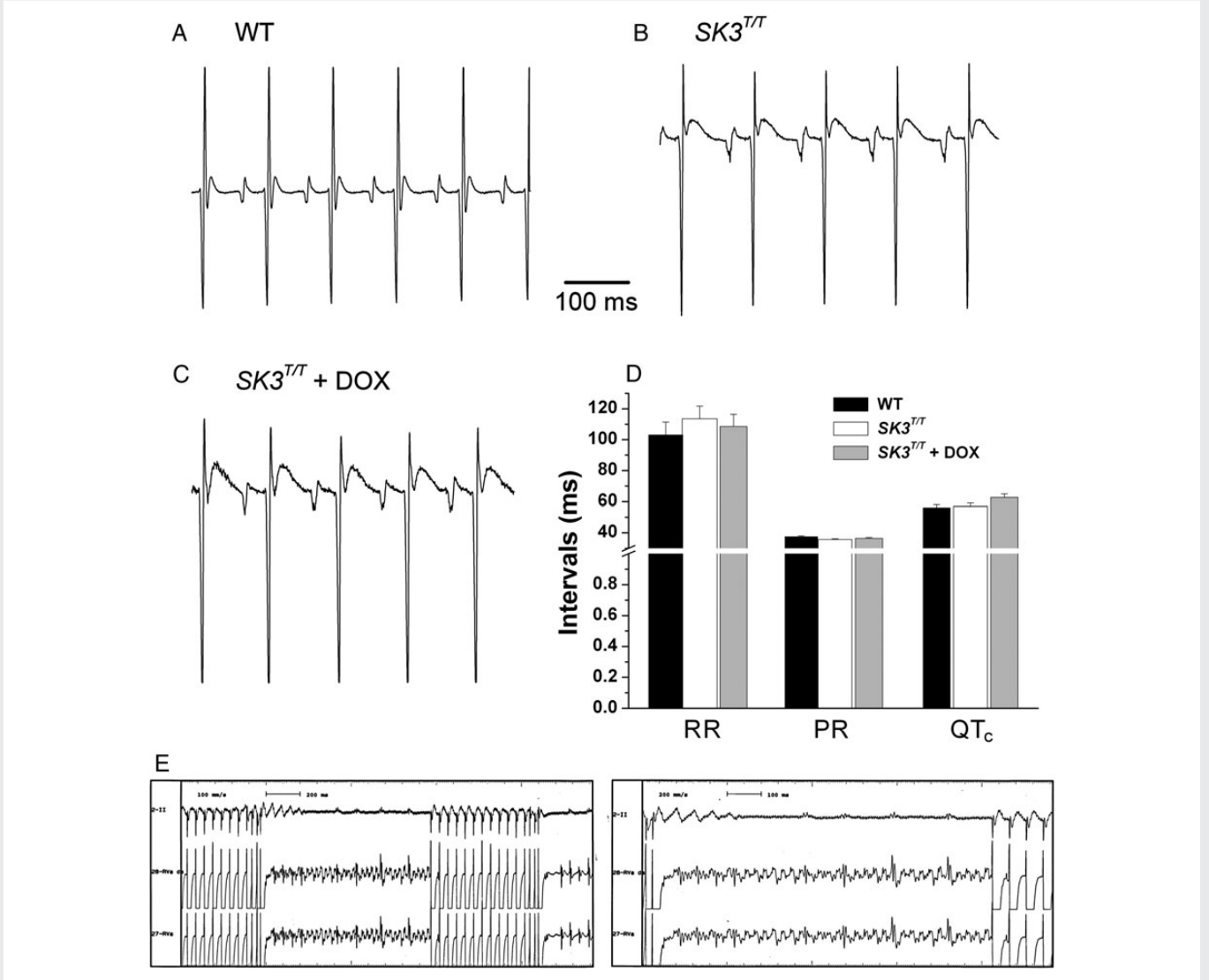

Figure 4 Functional roles of SK3 channels in the intact heart assessed using $SK3^{T/T}$ mice. (*A–C*) Examples of ECG recorded from the three different groups of mice including WT, and $SK3^{T/T}$ with and without treatment with DOX. (*D*) Summary data for RR, PR, and QT_c intervals ($n = 6$ animals for each group). No significant differences were detected in the three groups of animals. (*E*) Examples of atrial fibrillation induced in *SK3* mutant animals using programmed stimulation.

Table 2 ***In vivo*** **electrophysiological studies in WT, SK3$^{+/T}$, and SK3$^{T/T}$ mice**

	WT ($n = 7$)	*SK3*$^{+/T}$ ($n = 8$)	*SK3*$^{T/T}$ ($n = 4$)
SCL	294 ± 28	277 ± 48	224 ± 43
SNRT (120)	366 ± 32	361 ± 39	375 ± 41
SNRT (100)	375 ± 30	360 ± 49	370 ± 32
SNRT (80)	364 ± 40	337 ± 43	334 ± 8
WCL	97 ± 5	98 ± 6	83 ± 3
AVNERP (120)	80 ± 8	70 ± 4	57 ± 6
AERP (120)	56 ± 3	47 ± 3*	37 ± 3*
VERP (120)	37 ± 2	43 ± 6	40 ± 4

Data shown represent mean ± SEM, in ms.
SCL, sinus cycle length; SNRT, sinus node recovery time; WCL, Wenchebach cycle length; AVNERP, AERP, and VERP refer to the effective refractory period for the atrioventricular node, atria, and ventricles, respectively; AVNERP, AERP, and VERP were performed using the basic cycle length of 120 ms; *n* refers to the number of the animals in the studies.
*$P < 0.05$.

shorter compared with the WT animals (*$P < 0.05$). Our previous data demonstrated an increase in AV node conduction in mice with SK2 overexpression,[16] *SK3* mutant mice show a trend towards increasing AV node conduction comparing WT, heterozygous, and homozygous mutant mice using Wenchebach cycle length (WCL) measurement (see *Table 2*). However, the shortening of the WCL was not statistically significant. More importantly, atrial arrhythmias, mainly atrial fibrillation, were induced in adult *SK3* mutant animals. In contrast, atrial arrhythmias were induced in none of the WT littermates. Indeed, previous studies using the same background mouse model have shown that WT mice were not inducible for atrial arrhythmias in the absence of carbachol. *Figure 4E* shows examples of atrial fibrillation induced in adult *SK3* mutant mice. The *in vivo* electrophysiological parameters from adult mice are summarized in *Table 2*.

4. Discussion

4.1 SK3 contributes towards atrial action potential repolarization

In this study, we directly tested the role of SK3 channel in atrial myocytes and also in the intact animals using *SK3*$^{T/T}$ mutant mice. The previous study has documented that, in the absence of DOX, the SK3 transcript and protein are overexpressed in *SK3*$^{T/T}$ mice.[26] Furthermore, SK3 channel expression can be suppressed by treatment with DOX.[26] We first confirmed the mutant model and demonstrated greater than 50-fold expression of the SK3 transcripts in both atria and ventricles of *SK3*$^{T/T}$ mice. Treatment with DOX decreased the transcript expression to less than half of the WT animals. *SK3*$^{T/T}$ mice show a significant decrease in survival compared with the heterozygous and WT littermates. On the other hand, the *SK3*$^{T/T}$ mice show normal cardiac function as assessed by echocardiography with no evidence of structural cardiac abnormalities.

Overexpression of SK3 channels results in a significant decrease in atrial APD mainly during late repolarization compared with WT littermates. Specifically, there is a significant decrease in APD_{90}, but not APD_{50} in *SK3*$^{T/T}$ mice. Treatment with DOX results in the prolongation of the APD_{90} in the atrial myocytes compared with *SK3*$^{T/T}$ mice. In addition, the responses to apamin are blunted in *SK3*$^{T/T}$ animals treated with DOX even though the expression of SK2 channel transcript is not significantly altered in *SK3*$^{T/T}$ animals. Taken together, the data suggest that SK2 and SK3 isoforms may form heteromultimers *in vivo*. Knockdown of SK3 isoform appears to decrease the apamin-sensitive SK2 current in *SK3*$^{T/T}$ animals treated with DOX. In addition, the findings suggest that both SK2 and SK3 isoforms contribute towards atrial action potential repolarization. Moreover, in contrast to the Ca^{2+}-activated K^+ channels (K_{Ca}) described in neurons, which underlie the afterhyperpolarization, in the heart, the currents contribute markedly towards the late phase of the cardiac repolarization. Overexpression of SK3 channels does not alter the resting membrane potentials of the atrial myocytes.

To further document the functional expression of the SK3 channel in the heart, we directly recorded $I_{K,Ca}$ using whole-cell, patch-clamp techniques. Our patch-clamp recordings are consistent with the notion that SK3 channels are expressed and contribute functionally in atrial myocytes. Finally, even though *SK3*$^{T/T}$ mice demonstrate a greater than 50-fold increase in the expression of SK3 transcripts, the current density recorded in *SK3*$^{T/T}$ mice shows only a four-fold increase compared with that of the WT, suggesting that the mRNA abundance does not directly translate into changes in protein abundance.

Finally, controversies exist regarding the roles of SK channels in the heart. Nagy *et al.*[25] reported that SK channels do not contribute to action potential repolarization in rat, dog, and human ventricular myocytes under normal physiological conditions. Several factors may contribute to the observed discrepancy. First, the authors used ventricular myocytes, which have been documented to express the lower level of SK channels; secondly, the recording pipette solution and the intracellular free calcium concentration in their study are different from which we have used in our study. Finally, the disparities noted may be due to species differences. Nonetheless, our previous published study documented the roles of SK channel in human atrial myocytes.[11] Further studies are necessary to elucidate the roles of these unique channels in the heart.

4.2 Clinical implications of the study

Atrial fibrillation represents one of the most common arrhythmia clinically and is associated with a significant risk of embolism and stroke. Moreover, the current treatment strategies have proved largely inadequate. There are exciting recent studies to support the genetic basis for atrial fibrillation. Indeed, genome-wide association studies have identified multiple risk loci that confer increased susceptibility to atrial fibrillation.[36–39] Among these loci, *KCNN3* has been identified as one of the susceptibility genes. Specifically, a common variant on chromosome 1q21 which is intronic to *KCNN3* gene has been associated with lone atrial fibrillation in several cohorts.[23,24]

Our study using *SK3*$^{T/T}$ mutant mice support distinct contribution of SK3 channels to the terminal repolarization of the APs in atrial myocytes. Overexpression or down-regulation of the SK3 channels result in abbreviation or prolongation of the atrial APs, respectively. Moreover, we have previously documented that different members of SK channels can co-assemble to form heteromultimers in human cardiac myocytes.[13] Hence, genetic variation in one isoform may affect the function of other isoforms and the overall $I_{K,Ca}$.

Even though the underlying mechanisms for atrial fibrillation are highly heterogeneous, several studies have identified mutations in ion channels

as possible causes of inherited atrial fibrillation (AF).[36,40–42] The gain-of-function mutations in K^+ channels are predicted to result in the decrease in APD and AERP leading to atrial fibrillation. On the other hand, a number of patients with the mutation also had a prolonged QT interval,[41] suggesting that delayed repolarization may also increase the susceptibility to atrial fibrillation.

4.3 Unique features of SK channels in atrial repolarization

Since SK channels are gated solely by changes in Ca_i^{2+}, the channels provide a direct link between changes in $Ca^{2+}{}_i$ and membrane potentials. An increase in Ca_i^{2+} during rapid atrial arrhythmias may produce profound changes in AP profiles via the Ca^{2+}-dependent channels. Indeed, during acute phase of paroxysmal atrial fibrillation, the rapid depolarization may increase Ca_i^{2+} and potentiate $I_{K,Ca}$, resulting in acute electrical remodelling with abbreviation of AP and maintenance of the arrhythmias. The phenomenon of electrical remodelling has been well documented in several models of atrial fibrillation. Recent studies have documented exciting roles of SK channel blockers in models of atrial fibrillation. Our present study helps to contribute to the knowledge gap regarding the contribution of SK3 in the repolarization of atrial myocytes. Additional studies are required to further investigate the mechanisms contributing to the sudden death in the homozygous mutant animals (see Supplementary material online).

Supplementary material

Supplementary material is available at *Cardiovascular Research* online.

Acknowledgements

We thank Dr Ebenezer N. Yamoah for helpful suggestions and comments.

Conflict of interest: none declared.

Funding

This work was funded by the National Institutes of Health Grants (HL85727 and HL85844), the Department of Veteran Affairs Merit Review Grant (I01BX000576), and the California Institute of Regenerative Medicine (RB4-05764). X.Z. was partially supported by the Academic Federation Innovative Development Awards from UC Davis (FS12XDZ).

References

1. Kohler M, Hirschberg B, Bond CT, Kinzie JM, Marrion NV, Maylie J *et al*. Small-conductance, calcium-activated potassium channels from mammalian brain. *Science* 1996;**273**:1709–1714.
2. Bond CT, Maylie J, Adelman JP. Small-conductance calcium-activated potassium channels. *Ann N Y Acad Sci* 1999;**868**:370–378.
3. Bond CT, Maylie J, Adelman JP. SK channels in excitability, pacemaking and synaptic integration. *Curr Opin Neurobiol* 2005;**15**:305–311.
4. Adelman JP, Maylie J, Sah P. Small-conductance Ca^{2+}-activated K^+ channels: form and function. *Annu Rev Physiol* 2011;**74**:245–269.
5. Vergara C, Latorre R, Marrion NV, Adelman JP. Calcium-activated potassium channels. *Curr Opin Neurobiol* 1998;**8**:321–329.
6. Kaczorowski GJ, Garcia ML. Pharmacology of voltage-gated and calcium-activated potassium channels. *Curr Opin Chem Biol* 1999;**3**:448–458.
7. Stocker M. Ca^{2+}-activated K^+ channels: molecular determinants and function of the SK family. *Nat Rev Neurosci* 2004;**5**:758–770.
8. Weatherall KL, Goodchild SJ, Jane DE, Marrion NV. Small conductance calcium-activated potassium channels: from structure to function. *Prog Neurobiol* 2010;**91**:242–255.
9. Weatherall KL, Seutin V, Liegeois JF, Marrion NV. Crucial role of a shared extracellular loop in apamin sensitivity and maintenance of pore shape of small-conductance calcium-activated potassium (SK) channels. *Proc Natl Acad Sci USA* 2012;**108**:18494–18499.
10. Ishii TM, Maylie J, Adelman JP. Determinants of apamin and d-tubocurarine block in SK potassium channels. *J Biol Chem* 1997;**272**:23195–23200.
11. Xu Y, Tuteja D, Zhang Z, Xu D, Zhang Y, Rodriguez J *et al*. Molecular identification and functional roles of a Ca^{2+}-activated K^+ channel in human and mouse hearts. *J Biol Chem* 2003;**278**:49085–49094.
12. Tuteja D, Xu D, Timofeyev V, Lu L, Sharma D, Zhang Z *et al*. Differential expression of small-conductance Ca^{2+}-activated K^+ channels SK1, SK2, and SK3 in mouse atrial and ventricular myocytes. *Am J Physiol Heart Circ Physiol* 2005;**289**:H2714–H2723.
13. Tuteja D, Rafizadeh S, Timofeyev V, Wang S, Zhang Z, Li N *et al*. Cardiac small conductance Ca^{2+}-activated K^+ channel subunits form heteromultimers via the coiled-coil domains in the C termini of the channels. *Circ Res* 2010;**107**:851–859.
14. Lu L, Zhang Q, Timofeyev V, Zhang Z, Young JN, Shin HS *et al*. Molecular coupling of a Ca^{2+}-activated K^+ channel to L-type Ca^{2+} channels via α-actinin2. *Circ Res* 2007;**100**:112–120.
15. Lu L, Timofeyev V, Li N, Rafizadeh S, Singapuri A, Harris TR *et al*. α-actinin2 cytoskeletal protein is required for the functional membrane localization of a Ca^{2+}-activated K^+ channel (SK2 channel). *Proc Natl Acad Sci USA* 2009;**106**:18402–18407.
16. Ozgen N, Dun W, Sosunov EA, Anyukhovsky EP, Hirose M, Duffy HS *et al*. Early electrical remodeling in rabbit pulmonary vein results from trafficking of intracellular SK2 channels to membrane sites. *Cardiovasc Res* 2007;**75**:758–769.
17. Sosunov EA, Anyukhovsky EP, Hefer D, Rosen TS, Danilo P Jr, Janse MJ *et al*. Region-specific, pacing-induced changes in repolarization in rabbit atrium: an example of sensitivity to the rare. *Cardiovasc Res* 2005;**67**:274–282.
18. Diness JG, Sorensen US, Nissen JD, Al-Shahib B, Jespersen T, Grunnet M *et al*. Inhibition of small-conductance Ca^{2+}-activated K^+ channels terminates and protects against atrial fibrillation. *Circ Arrhythm Electrophysiol* 2010;**3**:380–390.
19. Diness JG, Skibsbye L, Jespersen T, Bartels ED, Sorensen US, Hansen RS *et al*. Effects on atrial fibrillation in aged hypertensive rats by Ca^{2+}-activated K^+ channel inhibition. *Hypertension* 2011;**57**:1129–1135.
20. Skibsbye L, Diness JG, Sorensen US, Hansen RS, Grunnet M. The duration of pacing-induced atrial fibrillation is reduced in vivo by inhibition of small conductance Ca^{2+}-activated K^+ channels. *J Cardiovasc Pharmacol* 2011;**57**:672–681.
21. Chua SK, Chang PC, Maruyama M, Turker I, Shinohara T, Shen MJ *et al*. Small-conductance calcium-activated potassium channel and recurrent ventricular fibrillation in failing rabbit ventricles. *Circ Res* 2011;**108**:971–979.
22. Chang PC, Turker I, Lopshire JC, Masroor S, Nguyen BL, Tao W *et al*. Heterogeneous upregulation of apamin-sensitive potassium currents in failing human ventricles. *J Am Heart Assoc* 2013;**2**:e004713.
23. Ellinor PT, Lunetta KL, Glazer NL, Pfeufer A, Alonso A, Chung MK *et al*. Common variants in KCNN3 are associated with lone atrial fibrillation. *Nat Genet* 2010;**42**:240–244.
24. Ellinor PT, Lunetta KL, Albert CM, Glazer NL, Ritchie MD, Smith AV *et al*. Meta-analysis identifies six new susceptibility loci for atrial fibrillation. *Nat Genet* 2012;**44**:670–675.
25. Nagy N, Szuts V, Horvath Z, Seprenyi G, Farkas AS, Acsai K *et al*. Does small-conductance calcium-activated potassium channel contribute to cardiac repolarization? *J Mol Cell Cardiol* 2009;**47**:656–663.
26. Bond CT, Sprengel R, Bissonnette JM, Kaufmann WA, Pribnow D, Neelands T *et al*. Respiration and parturition affected by conditional overexpression of the Ca^{2+}-activated K^+ channel subunit, SK3. *Science* 2000;**289**:1942–1946.
27. Hammond RS, Bond CT, Strassmaier T, Ngo-Anh TJ, Adelman JP, Maylie J *et al*. Small-conductance Ca^{2+}-activated K^+ channel type 2 (SK2) modulates hippocampal learning, memory, and synaptic plasticity. *J Neurosci* 2006;**26**:1844–1853.
28. Li N, Timofeyev V, Tuteja D, Xu D, Lu L, Zhang Q *et al*. Ablation of a Ca^{2+}-activated K^+ channel (SK2 channel) results in action potential prolongation in atrial myocytes and atrial fibrillation. *J Physiol* 2009;**587**:1087–1100.
29. Tuteja D, Xu D, Timofeyev V, Lu L, Sharma D, Zhang Z *et al*. Differential isoform expression of small conductance Ca^{2+}-activated K^+ channels, SK1, SK2 and SK3 channels in mouse atrial and ventricular myocytes. *Am J Physiol Heart Circ Physiol* 2005;**289**:H2714–H2723.
30. Hamill OP, Marty A, Neher E, Sakmann B, Sigworth FJ. Improved patch-clamp techniques for high-resolution current recording from cells and cell-free membrane patches. *Pflugers Arch* 1981;**391**:85–100.
31. Robertson S, Potter JD. The regulation of free Ca^{2+} ion concentration by metal chelators. In: Schwartz A, ed. *Methods in Pharmacology-Myocardial Biology*. New York: Springer US; 1984. p63–75.
32. Zhang Z, Xu Y, Song H, Rodriguez J, Tuteja D, Namkung Y *et al*. Functional roles of $Ca_v1.3$ (α_{1D}) calcium channel in sinoatrial nodes: insight gained using gene-targeted null mutant mice. *Circ Res* 2002;**90**:981–987.
33. Mitchell GF, Jeron A, Koren G. Measurement of heart rate and Q-T interval in the conscious mouse. *Am J Physiol* 1998;**274**:H747–H751.
34. Zhang Z, He Y, Tuteja D, Xu D, Timofeyev V, Zhang Q *et al*. Functional roles of $Ca_v1.3$ (α_{1D}) calcium channels in atria: insights gained from gene-targeted null mutant mice. *Circulation* 2005;**112**:1936–1944.
35. Berul CI, Aronovitz MJ, Wang PJ, Mendelsohn ME. In vivo cardiac electrophysiology studies in the mouse. *Circulation* 1996;**94**:2641–2648.
36. Ellinor PT, Macrae CA. The genetics of atrial fibrillation. *J Cardiovasc Electrophysiol* 2003;**14**:1007–1009.

37. Ellinor PT, Shin JT, Moore RK, Yoerger DM, MacRae CA. Locus for atrial fibrillation maps to chromosome 6q14–16. *Circulation* 2003;**107**:2880–2883.
38. Sinner MF, Ellinor PT, Meitinger T, Benjamin EJ, Kaab S. Genome-wide association studies of atrial fibrillation: past, present, and future. *Cardiovasc Res* 2011;**89**:701–709.
39. Magnani JW, Rienstra M, Lin H, Sinner MF, Lubitz SA, McManus DD *et al*. Atrial fibrillation: current knowledge and future directions in epidemiology and genomics. *Circulation* 2011; **124**:1982–1993.
40. Brugada R, Tapscott T, Czernuszewicz GZ, Marian AJ, Iglesias A, Mont L *et al*. Identification of a genetic locus for familial atrial fibrillation. *N Engl J Med* 1997;**336**: 905–911.
41. Chen YH, Xu SJ, Bendahhou S, Wang XL, Wang Y, Xu WY *et al*. KCNQ1 gain-of-function mutation in familial atrial fibrillation. *Science* 2003;**299**:251–254.
42. Hong K, Bjerregaard P, Gussak I, Brugada R. Short QT syndrome and atrial fibrillation caused by mutation in KCNH2. *J Cardiovasc Electrophysiol* 2005;**16**:394–396.